

The Galaxy structure across the Vela Gum

E.E. Giorgi^{1,2}, M.S. Pera^{2,3}, G. Perren^{2,3}, R.A. Vázquez^{1,2}, G.R. Solivella^{1,2} & A. Cruzado^{1,2}

¹ *Facultad de Ciencias Astronómicas y Geofísicas, UNLP, Argentina*

² *Instituto de Astrofísica de La Plata, CONICET-UNLP, Argentina*

³ *Facultad de Ciencias Exactas, Ingeniería y Agrimensura, UNR, Argentina*

Contact / egiorgi@fcaglp.unlp.edu.ar

Resumen / Presentamos los primeros resultados preliminares de un estudio sobre la población de cúmulos abiertos vista en dirección a la Nebulosa Gum. Se trata de una estructura de gas de emisión muy grande y cercana que abarca desde $l=240^\circ$ hasta $l=270^\circ$ y desde $b=+8^\circ$ hasta $b=-15^\circ$, aproximadamente. Aprovechando la impresionante precisión y profundidad ($G \approx 20$) de los datos proporcionados por la misión *Gaia* (EDR3) y que ahora tenemos dos poderosas herramientas para un análisis automatizado de datos de cúmulos abiertos, ASteCA y pyUPMASK, iniciamos un proyecto destinado a reanalizar los parámetros fundamentales de varias docenas de cúmulos abiertos ubicados en el área de la Nebulosa Gum.

Abstract / We present first and preliminary results of a study on the open cluster population seen against the Gum Nebula. This is a very large and nearby emission gas structure covering from $l=240^\circ$ to $l=270^\circ$ and from $b=+8^\circ$ to $b=-15^\circ$, approximately. Taking advantage of the impressive precision and depth ($G \approx 20$) of data provided by the *Gaia* mission (EDR3) and that we have now two powerful tools for an automated analysis of open clusters data, ASteCA and pyUPMASK, we started a project aimed at reanalyzing the fundamental parameters of several dozens of open clusters located in the Gum Nebula area.

Keywords / Galaxy: structure — open clusters and associations: general

1. Introduction

The *Gaia* mission (Gaia Collaboration et al., 2016) offers us a large amount of stellar data in our galaxy. The latest EDR3 data release (Riello et al., 2021) provides G magnitude and colors for more than 1.8 billion stars including sky positions, parallaxes, and proper motions for sources down to $G \approx 20$. It is then possible to perform all kind of studies, from modest -in size- structures (individual stars, star associations, star clusters, etc.) to those ones concerning large structures such as galaxy arms. As for the region of our interest -the whole Vela Gum area- it contains prominent astronomical structures projected against its areal surface such as the Vela OB2 and OB1 associations, the Vela Supernovae Remnant, the Vela Pulsar and the Vela Molecular Ridge. The emission region overlaps too with the IRAS Vela Shell located close to the south. The stellar population connected with some of these features has been examined recently (Cantat-Gaudin et al., 2019). However, a reanalysis of the fundamental parameters of open clusters is urgently needed if we want to have an improved picture of the galaxy substructures beyond the Gum Nebula (e.g. confirming the Perseus arm existence). To handle *Gaia* data in Gum Nebula, we have specific computational tools to analyze them without requiring personal supervision and thus obtain homogeneous results (Perren et al., 2015); (Pera et al., 2021).

2. The data

Parallaxes, proper motions, G magnitudes, and colors (B_p - R_p) for cluster stars in the Vela Gum were down-

loaded for 52 out of about two hundred clusters under investigation. A script was used to query all data in the EDR3 catalog within a circle centered on the published coordinates of each cluster.

3. Description of the method

Cluster by cluster, an analysis of membership was made with pyUpmask ((Pera et al., 2021)), a python code that has been designed to distinguish between member and non-member stars of a cluster. This is, the process yields the individual probability that the star is a cluster member. Previously, stellar parallaxes were corrected using the procedures described in (Lindgren et al., 2021).

Those stars with the highest probabilities were then analyzed using the ASteCA code ((Perren et al., 2015)) to get the fundamental cluster parameters (age, distance, mean proper motions and color excess, total mass and metal content). ASteCA does this, by comparing the color-magnitude diagrams of likely members with synthetic clusters from Parsec ((Bressan et al., 2012)). The procedure implies thousand iterations.

As an example, we show in Fig. 1 the estimation of mean cluster parallax and the best fitting with synthetic clusters for NGC 2818 (upper panels) and Melotte 66 (lower panels). The red isochrone curve is for visual guidance only and means that there is no fit. In Table 1 we inform the results for 52 open clusters, where the second column shows the cluster distance from our mean parallax, the fifth column is for the ASteCA analysis, the sixth for distances from (Dias et al., 2021) and

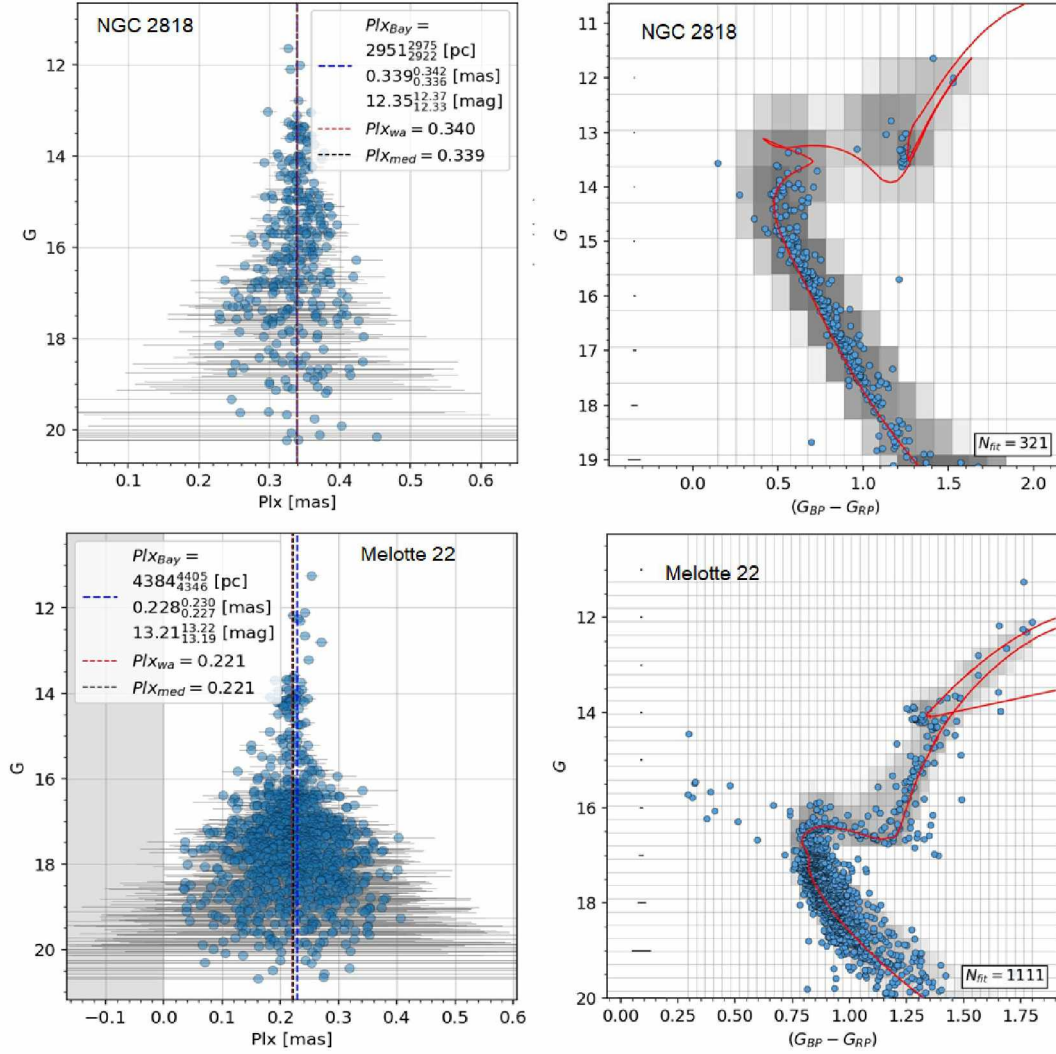


Figure 1: Parallax and photometric analysis for NGC 2818 (upper panels) and Melotte 66 (lower pannels). Plx_{Bay} indicates the Bayes parallax, Plx_{wa} is the parallax weighted average and Plx_{med} the median.

the seventh is the $\log(\text{age})$ of the cluster calculated by ASteCA.

4. Conclusions

In this article we present the first and very preliminary results of a study based on the re-analysis of many open clusters projected against the Gum Nebula. Our project will continue with the study of all the clusters detected in this region, currently around 200, which will allow us to complete an improved image of the substructures of the galaxy beyond the Gum Nebula.

Acknowledgements: This work has made use of data from the European Space Agency (ESA) mission *Gaia* (<https://www.cosmos.esa.int/gaia>), processed by the *Gaia* Data Processing and Analysis Consortium (DPAC, <https://www.cosmos.esa.int/web/gaia/dpac/consortium>). Funding for the DPAC has been provided by national institutions, in particular the institutions participating in the *Gaia* Multilateral Agreement.

References

References

Bressan A., et al., 2012, MNRAS, 427, 127
 Cantat-Gaudin T., et al., 2019, A&A, 626, A17
 Dias W.S., et al., 2021, MNRAS, 504, 356
 Gaia Collaboration, et al., 2016, A&A, 595, A1
 Lindegren L., et al., 2021, A&A, 649, A4
 Pera M.S., et al., 2021, A&A, 650, A109
 Perren G.I., Vázquez R.A., Piatti A.E., 2015, A&A, 576, A6
 Riello M., et al., 2021, A&A, 649, A3

Table 1: Distances in pc calculated with parallax (dPlx) and with photometry (dPhot). Proper motions in right ascension (pmra) and declination (pmd). D represents the distances in pc from (Dias et al., 2021). Age calculated for the open clusters under investigation ($\log t$) is indicated.

CLUSTER	dPlx	pmra	pmd	dPhot	D	$\log t$
TRUMPLER 9	2500	-3.4	3.1	2517	2907	8.0
HAFFNER 19	4160	-2.6	2.7	3197	6289	7.1
NGC 2453	4011	-2.4	3.4	3661	4545	8.2
HAFFNER 14	3603	-1.8	1.8	3075	4329	8.4
NGC 2483	3955	-2.3	3.3	3936	–	8.4
HAFFNER 21	3044	-1.4	1.6	3093	3534	8.7
RUPRECHT 35	3443	-2.3	3.2	2824	4098	8.4
NGC 2489	1882	-2.5	2.2	1767	2128	8.7
HAFFNER 22	2567	-1.6	3.0	2893	3021	9.3
HAFFNER 17	3267	-1.2	1.9	1964	4115	8.6
HAFFNER 15	3416	-2.2	3.3	2758	4237	8.1
RUPRECHT 50	2245	-1.8	2.4	3129	2421	8.3
RUPRECHT 47	3337	-2.5	2.7	3062	4149	8.5
NGC 2571	1279	-4.9	4.3	1099	1383	8.0
RUPRECHT 48	3471	-2.5	2.9	3597	4132	8.3
RUPRECHT 52	3603	-2.5	2.8	5686	–	8.4
NGC 2587	2911	-4.2	3.6	2703	3300	8.7
HAFFNER 26	2770	-1.6	2.4	3276	3279	8.7
NGC 2567	1648	-2.9	2.7	1809	1855	8.7
NGC 2580	3950	-2.3	1.9	4607	5102	8.8
RUPRECHT 31	4146	-1.6	2.0	9020	–	9.6
RUPRECHT 58	2962	-2.6	1.4	3568	3745	8.6
NGC 2627	1705	-2.3	3.0	2360	1916	8.6
NGC 2588	4228	-1.9	2.6	4432	5181	8.8
RUPRECHT 59	4581	-2.6	3.2	5508	–	8.0
RUPRECHT 61	3357	-2.5	3.8	3293	3584	9.0
RUPRECHT 152	4549	-1.3	2.2	10725	–	8.6
NGC 2477	1388	-2.4	0.8	1208	1499	9.1
ASCC 45	3699	-2.9	3.2	4615	–	8.3
NGC 2658	3831	-2.4	2.3	4009	5076	8.8
NGC 2579	4118	-2.5	3.2	5174	–	8.3
NGC 2635	4595	-2.5	2.2	4831	6944	8.5
RUPRECHT 68	2778	-2.6	5.6	2661	3322	9.3
PISMIS 3	2123	-4.7	6.7	1407	2463	9.5
RUPRECHT 66	3668	-3.1	3.1	4098	4484	9.1
PISMIS 2	3613	-4.7	5.4	2213	–	9.6
PISMIS 7	4578	-3.3	2.8	3727	6667	9.0
PISMIS 5	909	-5.4	4.5	817	963	7.4
RUPRECHT 72	4252	-3.5	3.3	7423	–	8.9
RUPRECHT 158	4111	-3.1	3.5	9298	–	8.3
MELOTTE 66	4392	-1.4	2.8	4630	5291	9.5
RUPRECHT 64	902	-5.6	3.7	692	–	7.2
NGC 2818	2947	-4.4	4.5	3138	3610	9.0
NGC 2671	1353	-1.5	1.0	808	1451	9.3
BH 37	3602	-3.5	4.0	3141	3922	8.7
RUPRECHT 74	3175	0.0	3.3	4375	–	9.1
RUPRECHT 60	4020	-3.8	5.5	5265	5376	8.8
NGC 2659	1879	-4.3	3.0	1555	2299	8.7
RUPRECHT 71	1877	-5.2	4.6	1862	2049	7.6
NGC 2670	1433	-5.3	3.7	1791	1536	7.8
COLLINDER 205	1777	-4.8	4.0	1269	2198	7.0